Multicriteria Algorithms with Applications

Journal Homepage: sciencesforce.com/mawa

Multicriteria Algo. Appl. Vol. 3 (2024) 50–59

Paper Type: Original Article

A Study of Neutrosophic Sets and Deep Learning Models for Breast Cancer Classification

Walid Abdullah [1,*]

[1] Department of Computer Science, Faculty of Computers and Informatics, Zagazig University, Zagazig 44519, Egypt; waleed@zu.edu.eg.

Received: 15 Dec 2023 **Revised:** 26 Mar 2024 **Accepted:** 24 Apr 2024 **Published:** 28 Apr 2024

Abstract

Medical image classification and detection using artificial intelligence (AI) can help enhance medical care services. Unfortunately, most medical image modalities suffer from some noise and uncertainty, which decreases the performance of disease detection and classification. Neutrosophic sets (NS) can handle uncertainty data within medical images. NS can present images into three subsets: true (T), indeterminacy (I), and fuzzy sets (FS). In this study, we investigate the performance of deep learning (DL) models under the NS domain for breast cancer classification. The crisp image domain is converted to the NS domain and represents the image into three subsets. The converted images are used to train seven DL models, such as VGG16, VGG19, ResNet50, ResNet150, DenseNest121, EfficientNetB2, and MobileNetV2. A comparison between DL under NS and on the FS, domain has been made in terms of accuracy, precision, recall, and F1 score. The experimental results showed superior results for NS over FS.

Keywords: Breast Cancer Classification, Neutrosophic Set (NS), Deep Learning (DL), Transfer Learning.

1 | Introduction

Breast cancer is one of the most common forms of cancer. It is thought to be the second most common cancer worldwide, right after lung cancer, and is considered the fifth most common reason for cancer death [1]. Breast cancer usually has no symptoms, so it's critical to detect it effectively [2]. The most prevalent type of breast cancer is invasive ductal carcinoma (IDC) [3]. Breast cancer can be scanned through various imaging methods, such as mammography, ultrasonography, and magnetic resonance imaging (MRI) [4, 5]. Identifying and classifying breast cancer subtypes accurately is a crucial clinical job, and automated techniques can be applied to cut down on errors and save time.

In recent years, artificial intelligence has rapidly developed and evolved in various fields, including healthcare fields [6, 7]. AI techniques such as deep learning (DL) methods, particularly convolutional neural networks (CNNs), have significantly impacted healthcare through image feature extraction and analysis. By leveraging large datasets of medical images, CNNs can automatically learn intricate patterns and features indicative of various diseases, including breast cancer. Through sophisticated feature extraction techniques, CNNs can identify subtle abnormalities in medical images with high accuracy, aiding in disease detection and diagnosis

Corresponding Author: waleed@zu.edu.eg

https://doi.org/10.61356/j.mawa.2024.3237

[8-11]. Unfortunately, medical images may contain data noise and uncertainty, which leads to imprecise information that may hinder accurate diagnosis and analysis [12].

The neutrosophic set (NS) logic idea was introduced by Florentin Smarandache in 1995 and unified and generalized in 1999 [13, 14]. is an extension of fuzzy set (FS) and classical logic to deal with uncertainty and imprecise information, FS is an extension of classical logic to enable reasoning under uncertainty or the degrees of truth between 0 and 1 [15, 16]. NS has been used in many computer science fields, including pattern recognition and preprocessing [17, 18], It helps with a variety of research and real-world problem-solving in many different fields, including medical [19].

In this study, we investigate the integration between the performance of different DL models under the NS domain for IDC classification. The evaluation of this study is done over 20000 images, divided into 10000 IDC positive and 10000 IDC negative images.

So, the contribution of this study can be concluded as follows:

i. The uncertainty was handled in three degrees of membership: true membership, indeterminacy membership, and falsity membership.

ii. The integration between the DL model and NS is achieved using seven different DL models such as VGG16, VGG19, ResNet50, ResNet150, DenseNest121, EfficientNetB2, and MobileNetV2.

iii. A comparison with FS is conducted in terms of accuracy, precision, recall, and F1 score.

iv. The NS shows superior results than FS with the DenseNest121 model.

The rest of the paper is structured as follows: Section 2 presents the literal review and related work of using FS and NS with DL techniques in medical fields, and Section 3 describes the utilized dataset and DL methods used in this study. Section 4 provides the experiment setup, experimental results, and discussions of the proposed models and other DL models for meat quality assessment and classification. The conclusion of this paper is presented in Section 5.

2 | Literature Review

In this section, we review relevant literature on the utilization of NS and FS membership functions with DL techniques in image classification. By examining previous studies, we aim to identify gaps and shortcomings and highlight key findings, methodologies, and achievements of combining NS and FS with DL models for different problems.

Since the NS has played a vital role in handling noisy images with uncertain or vague information, Authors in [20] proposed a novel NS-based DL method for the analysis of digital mammograms for detecting and classifying microcalcifications (MCs), which are important signs of breast cancer at an early stage. Membership sets of NS are used for mapping digital mammograms in three NS domains named T, I, and F. These domains were used to train a CNN model for conducting a set of tasks, including lesion detection, regional clustering, and image classification. A neutrosophic reinforcement sample learning strategy (NRSL) is applied during the model training phase to speed up the training procedure. The obtained results showed that the proposed method achieved a sensitivity of 92.5%. For cluster-based MC detection assessment and area under the curve (AUC) on the validation and testing sets of 0.908 and 0.872, for case-based classification evaluation, these results demonstrated the effectiveness of combining the NS with DL techniques for automated detection and classification of MC clusters (MCC) in digital mammography images.

In [21], A study of the significance of NS on DL models was presented. The study was conducted on a limited COVID-19 x-ray dataset. The images are converted to the NS domain, which consists of three types of images: true (T) images, indeterminacy (I) images, and false (F) images. Then, the converted images are used to train different DL models. In this study, three DL models named Alexnet, Googlenet, and Restnet18 were trained and tested in the four domains of images: the original images against three NS subsets, and the results

were compared in terms of accuracy, precision, recall, and F1 score. The obtained results of the study showed that NS combined with DL models could be a promising step toward improving test accuracy, particularly considering the scarcity of COVID-19 datasets.

Authors in [22], proposed a neutrosophic multiple deep convolution neural network (NMDCNN) model for detecting skin cancer disease. In this model, the Neutrosophic Similarity Score (NSS) is used to determine the reinforced training number for each epoch until all epochs are finished during the training process. The images are classified into two types: benign and malignant. The obtained results demonstrated the competency of the proposed model. And proved the ability of the NNS method to select the best parameter in the learning process that led to the height's performance.

A new deep neural network model based on Neutrosophic Features for Skin Cancer Diagnosis is proposed in [23]. The proposed classifier model was trained and tested over various datasets, including PH2, ISIC 2017, 2018, and 2019. In this model, the NS technique used for suspected lesions is segmentation, which helps reduce noise and increase classification accuracy. The proposed model yields an accuracy mark of 99.50%, 99.33%, 98.56%, and 98.04% for the mentioned datasets, respectively, which is better than most of the pre-existing classifiers. these datasets in the segmentation task. On the other hand, A FS-based image segmentation model is proposed in [24] for melanoma detection, which is a type of skin cancer. FS was combined with a modified DL model called You Look Only Once (YOLO), which is based on a deep convolutional neural network (DCNN) to identify melanoma lesions from digital and dermoscopic lesions. The ISIC 2017 and ISIC 2018 dermoscopic image datasets are used to train the classifier, while the PH2 datasets and the two previously stated datasets are utilized to test the suggested algorithm. According to experimental results, the proposed model achieved an accuracy of 98.50, 96.17, and 95.9 for ISIC 2018, 2019, and PH2, respectively.

Furthermore, FS is utilized in [25] for the early detection of COVID-19 pneumonia using chest X-rays. FS was combined with a DL model, which is used for the extraction of useful feathers from FS images generated by a fuzzy edge detection algorithm. The obtained results showed that, compared to benchmark DL approaches, the suggested model produces a greater classification performance (accuracy rate of up to 81%).

A new technique for the automatic semantic segmentation (SS) of tumors in breast ultrasound (BUS) pictures combines FS and DL was proposed in [26]. The proposed approach comprises two steps: a convolutional neural network (CNN)-based SS and a FL-based preprocessing. The model was trained and tested on a small dataset of BUS. However, the obtained results were very impressive. There have been three quantitative performance evaluation metrics used: mean BF (Boundary F1) score, mean Jaccard index (mean intersection over union; IoU), and global accuracy (GA). The suggested model produced the best results over the 400 malignant BUS photos, with a mean IoU of 78.70% instead of 49.61%, a mean BF score of 68.08% instead of 42.63%, and a GA of 95.45% instead of 86.08% without the use of an FS preprocessing phase. Also, compared to simply using CNN-based SS, the segmented images that were produced could more accurately identify the locations of tumors.

Previous studies have advanced the use of FS and NS in DL methods with uncertainty and noise. However, there remains a need for robustness, and some of these studies lack high accuracy. and some of the other studies were conducted with a small dataset, which makes the results unpredictable in the long term. In addition, there are not enough studies that have performed a comparison between the results of FS and NS when combined with DL in the medical field.

3 | Materials and Methods

In this study, NS domain images and FS images are used to train a transfer DL model to detect IDC breast cancer. Then the models are tested, evaluated, and compared against each other. To study and compare the performance of different DL models on NS and FS images, this study will be conducted through various steps, as shown in Figure 1.

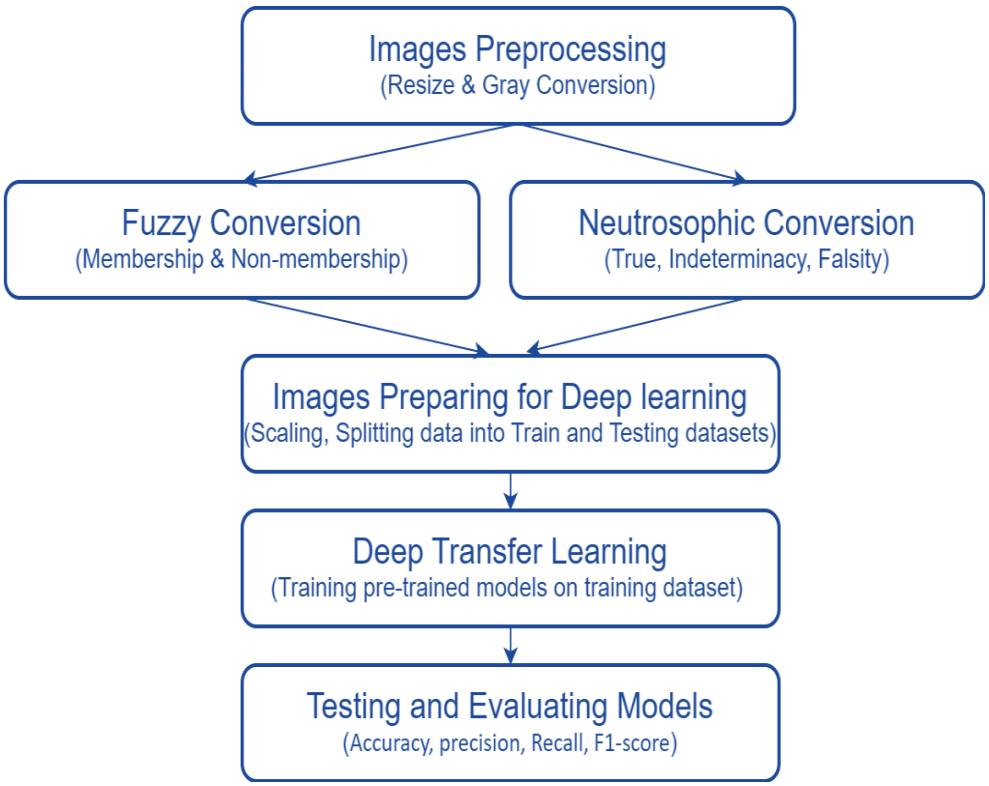

Figure 1. Main steps of the study.

3.1 | Utilized Dataset

A breast histogram image dataset is used for detecting IDC, which is the most common subtype of all breast cancers. The dataset was made up of 162 whole-mount slide photographs of breast cancer (BCa) specimens that were scanned at a magnification of 40x. 277,524 50×50 patches were taken out of that. The data was divided into 198,738 IDC negatives and 78,786 IDC positives [27].

In this study, sample data from the breast histogram images is utilized. The utilized data contains 20000 images, divided into 10000 IDC positive and 10000 IDC negative images. The images are converted through NS and FS, as discussed before. The converted images will be used to train the DL models to correctly classify the histogram images into two classes (IDC negative or IDC positive).

3.2 | Fuzzy Set (FS)

FS is a type of many-valued logic that deals with approximations. It is an extension of classical logic to enable reasoning under uncertainty, or the degrees of truth between 0 and 1, depending on a membership function that provides each element with a degree of membership, which defines how items belong to FS [15, 16].

FS conversion of images in membership and non-membership usually entails converting the image's pixel values into FS that indicate each pixel's degree of membership to categories. This process consists of three phases:

i. Fuzzification: Map the values of the pixel intensity to FS. In this step, membership functions are defined, giving each pixel value for the categories a degree of membership.

ii. Fuzzy inference: Determine each pixel's degree of membership in each category using fuzzy rules.

iii. Defuzzification: Transform the fuzzy output into crisp numbers. In order to identify each pixel's final category membership.

In this study, A triangular membership function is used to define how each pixel belongs to FS in image converting [28]. It is mathematically represented in Eqs. (1-2).

$$A = \{(x, \mu_A(y) | \, x \in U)\} \quad (1)$$

$$\mu(x; a, b, c) = \max(\min((x-a)/(b-a), (c-x)/(c-b)), 0) \quad (2)$$

Where $\mu_A(y)$ is the membership function in FS *A,* and *U* is the universe of discourse. *a, b, and c are* the minimum value, peek value, and maximum value membership function respectively. Figure 2 shows the difference between the original image and the FS-converted images.

(A) (B) (C)

Figure 2. Images Fuzzy Conversion (A) original image, (B) membership image, (C) non-membership image.

3.3 | Neutrosophic Set (NS)

NS is an extension of FS and classical logic. It is used to deal with uncertainty and imprecise situations. It was introduced by Florentin Smarandache[13, 14]. In Neutrosophic logic, each element of a set has three components:

i. True component (T): Denotes the percentage of how much the element belongs to the set.

ii. Indeterminate component (I): This represents the degree of uncertainty or the lack of information.

iii. Falsehood component (F): Denotes the degree to which an element does not belong to the set.

In the neutrosophic domain image conversion process, each pixel of an image is preprocessed by NS to calculate its T, F, I component values to detect which domain it belongs. in this process, Each Pixel in the image is represented as $P(i,j)$, and its NS domain percentages are represented as $P_{NS}(i,j) = \{T(i,j), I(i,j), F(i,j)\}$. Then T(i,j), I(i,j), and F(i,j) components can be computed as shown in Eqs. (3-6).

$$T(i,j) = \frac{\overline{g}(i,j) - \overline{g}_{min}}{\overline{g}_{max} - \overline{g}_{min}} \quad (3)$$

$$I(i,j) = \frac{H(i,j) - H_{min}}{H_{max} - H_{min}} \quad (4)$$

$$H(i,j) = abs(g(i,j) - \overline{g}(i,j)) \quad (5)$$

$$F(i,j) = 1 - T(i,j) \quad (6)$$

Where $g(i,j)$ represents a gray value of the related pixel, $\overline{g}(i,j)$ represent the region average value of $g(i,j)$, and $H(i,j)$ is the homogeneity value which is the absolute value of the difference between intensity $g(i,j)$ and its local mean value $\overline{g}(i,j)$. After the conversion of the image to the NS domain, the IDC (object) should be kept in the T domain, the edges be in the I domain, and the background should be kept in the F domain Figure 3 shows the difference between original image and the images after the conversion NS image domains.

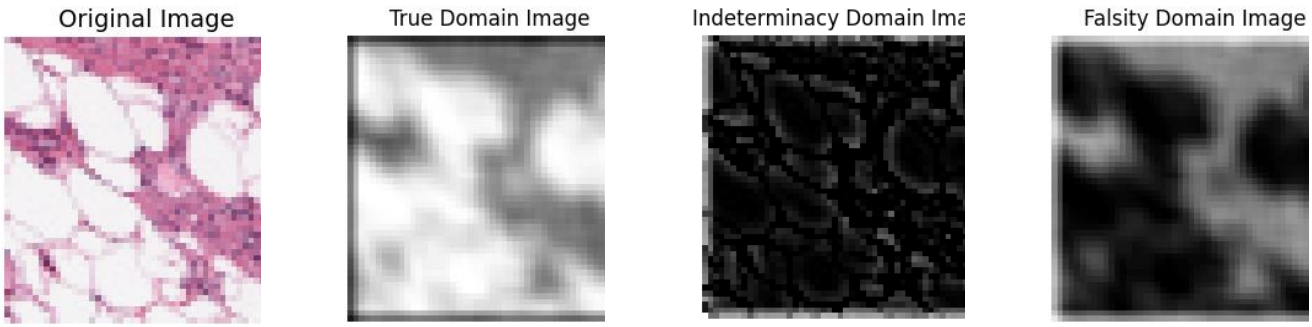

(A) (B) (C) (D)

Figure 3. Different NS Images Domains Conversion (a) Original images, (b) True domain, (c) Indeterminacy domain, and (d) Falsity domain image.

3.4 | Deep Learning (DL) Models

Transfer learning is a popular DL technique in which a pre-trained model on a certain task is utilized as a basis for another task [29]. This pre-trained model was trained on a huge dataset and learned to extract useful features from these images. So, use transfer learning to enhance your DL model's performance and speed training.

The different utilized DL models:

- VGG16, VGG19 [30].
- ResNet50, ResNet152 [31] .
- DenseNest121 [32].
- EfficientNetB0 [33].
- MobileNetV2 [34].

All utilized DL models are based on the Convolution Neural Network (CNN), which is a powerful model that is primarily used for image recognition and classification tasks [35]. Convolutional layers use a set of learnable filters, also known as kernels, to conduct convolutions on the input image to extract significant characteristics like textures, edges, and patterns. CNNs have demonstrated cutting-edge capabilities in a range of computer vision tasks.

4 | Experiments, Results, and Discussion

As mentioned above, in this study, A set of 7 popular pre-trained models were used for this task. These models are VGG16, VGG19, ResNet50, ResNet152, DenseNet121, EfficientNetB0, and MobileNetV2. All models were trained on the images produced via NS into T, I, and F domain images and FL into membership and non-membership images. The models use using Adam optimizer with a learning rate of 0.001 [8], a number of epochs equal to 50, and a batch size of 64 [9].

4.1 | Experiments Setup

The conversion of images to NS domain images was implemented using a software package (MATLAB), The experiments with DL models were conducted on the Kaggle platform with GPU Nvidia Tesla P100 With Ram 16 GB, the proposed model was developed and trained using Python version 3.10, Keres version 3.5 [36], and TensorFlow version 2.15 [37].

4.2 | Evaluation Metrics

To evaluate the proposed model and compare it against other state-of-art a set of metrics are used such as Accuracy, precision, recall, and F1-score which are mathematically represented in Eqs. (7-10).

- Accuracy – Measures the ratio of the number of correct predictions for all categories to the total number of predictions.

$$Accuracy = \frac{(TP + TN)}{(TP + FP + TN + FN)} \quad (7)$$

- Precision – The ratio of the number of correct predictions for a category to the total number of predictions in the same category.

$$Precision = \frac{TP}{(TP + FP)} \quad (8)$$

- Recall – Measures the proportion of correctly identified predictions for a category to the total number of identified predictions in the same category.

$$Recall = \frac{TP}{(TP + FN)} \quad (9)$$

- F1 Score – is the harmonic mean of precision and recall.

$$F1\ Score = 2 \times \frac{recall \times precision}{recall + precision} \quad (10)$$

4.3 | Experimental Results and Discussion

In this section, the performance of the transfer learning model was evaluated on utilized image data and compared against each other across the accuracy, precision, recall, and F1-score evaluation metrics. Tables 1 and 2 show model performance for FS images, membership, and non-membership images respectively. Tables 3,4 and 5 show the models' performance for the NS domain images T, I, and F domain images respectively.

Table 1. DL models performance for the membership fuzzy images.

	Model	Accuracy %	Precision %	Recall %	F1 Score %
1	VGG16	74.72	75	75	75
2	VGG19	74.37	75	74	74
3	ResNet50	69.24	70	69	69
4	ResNet152	72.92	73	73	73
5	DenseNest121	**74.82**	**75**	**75**	**75**
6	EfficientNetB0	71.79	72	72	72
7	MobileNetV2	74.04	74	74	74

Table 2. DL models performance for the non-membership fuzzy images.

	Model	Accuracy %	Precision %	Recall %	F1 Score %
1	VGG16	75.99	76	76	76
2	VGG19	75.99	76	76	76
3	ResNet50	73.19	73	73	73
4	ResNet152	71.37	72	73	73
5	DenseNest121	**76.09**	**76**	**76**	**76**
6	EfficientNetB0	73.22	73	73	73
7	MobileNetV2	72.37	72	72	72

Table 3. DL models performance for the true neutrosophic domain data.

	Model	Accuracy %	Precision %	Recall %	F1 Score %
1	VGG16	73.04	73	73	73
2	VGG19	72.57	73	73	71
3	ResNet50	63.75	70	64	61
4	ResNet152	71.57	72	72	71
5	DenseNest121	69	71	69	68
6	EfficientNetB0	**76.74**	**77**	**77**	**76**
7	MobileNetV2	71.79	72	72	72

Table 4. DL models performance for the intermediate neutrosophic domain data.

	Model	Accuracy %	Precision %	Recall %	F1 Score %
1	VGG16	73.90	74	74	74
2	VGG19	73.93	74	74	74
3	ResNet50	76.82	77	77	77
4	ResNet152	75.15	75	75	75
5	DenseNest121	**79.07**	**79**	**79**	**79**
6	EfficientNetB0	73.72	74	74	74
7	MobileNetV2	74.55	75	75	75

Table 5. DL models performance for the falsity of neutrosophic domain data.

	Model	Accuracy %	Precision %	Recall %	F1 Score %
1	VGG16	70.24	70	70	70
2	VGG19	71.27	71	71	71
3	ResNet50	75.84	76	76	75
4	ResNet152	73.90	74	74	74
5	DenseNest121	**76.09**	**76**	**76**	**76**
6	EfficientNetB0	74.84	75	75	75
7	MobileNetV2	69.02	69	69	69

The experiment's results concluded that, in terms of comparison between NS domain images and FS images, The NS domain images achieved a higher test accuracy than FS images. In terms of comparison between the T, I, and F NS domain images, the Indeterminacy (I) NS domain achieved the highest possible testing accuracy in all experiment trials. In terms of comparison between Transfer learning models, the DenseNest121 model has achieved the highest performance across all of the image types. Except for the True NS domain. Finally, the best accuracy of a model for an image type was shown in Table 4, where the DenseNest121 model achieved a 77.07 % accuracy and 77 % for precision and recall on Intermediate NS Domain images

5 | Conclusion and Future Directions

This study introduces a novel approach for improving the accuracy of invasive ductal carcinoma (IDC) classification in breast cancer using an integration between neutrosophic set (NS) and deep learning (DL) methods. Seven DL models have been developed to investigate their performance under the NS domain. NS can handle uncertainty and fuzziness in higher dimensions. DL is a more powerful tool for classification than traditional machine learning (ML) models. The evaluation of our study has been done over 20000 images to classify breast cancer disease. Finally, the NS shows superior results than the fuzzy set (FS) in terms of precision, recall, and F1 score.

In the future, more efforts are needed.

In this study, we observe that using NS for repeated image enhancement might blur the input image, resulting in a loss of detail. So, more efforts are needed to avoid blurring problems in NS-based techniques.

Acknowledgments

The author is grateful to the editorial and reviewers, as well as the correspondent author, who offered assistance in the form of advice, assessment, and checking during the study period.

Funding

This research has no funding source.

Data Availability

The datasets generated during and/or analyzed during the current study are not publicly available due to the privacy-preserving nature of the data but are available from the corresponding author upon reasonable request.

Conflicts of Interest

The authors declare that there is no conflict of interest in the research.

Ethical Approval

This article does not contain any studies with human participants or animals performed by any of the authors.

References

[1] Montazeri, A., Health-related quality of life in breast cancer patients: a bibliographic review of the literature from 1974 to 2007. Journal of experimental & clinical cancer research, 2008. 27: p. 1-31.
[2] Society, A.C., Breast cancer facts & figures 2019–2020. Am. Cancer Soc., 2019: p. 1-44.
[3] Goh, C.W., et al., Invasive ductal carcinoma with coexisting ductal carcinoma in situ (IDC/DCIS) versus pure invasive ductal carcinoma (IDC): a comparison of clinicopathological characteristics, molecular subtypes, and clinical outcomes. Journal of cancer research and clinical oncology, 2019. 145: p. 1877-1886.
[4] Sadoughi, F., et al., Artificial intelligence methods for the diagnosis of breast cancer by image processing: a review. Breast Cancer: Targets and Therapy, 2018. 10(null): p. 219-230.
[5] Andreea, G.I., et al., The role of imaging techniques in diagnosis of breast cancer. Curr Health Sci J, 2011. 37(2): p. 241-248.
[6] Gavrilova, Y., Artificial Intelligence vs. Machine Learning vs. Deep Learning: Essentials, 2020.
[7] Deepa, N., et al., An AI-based intelligent system for healthcare analysis using Ridge-Adaline Stochastic Gradient Descent Classifier. The Journal of Supercomputing, 2021. 77: p. 1998-2017.
[8] Salehi, A.W., et al., A study of CNN and transfer learning in medical imaging: Advantages, challenges, future scope. Sustainability, 2023. 15(7): p. 5930.
[9] Chowdhury, S.R., Y. Khare, and S. Mazumdar, Classification of diseases from CT images using LSTM-based CNN, in Diagnostic Biomedical Signal and Image Processing Applications with Deep Learning Methods. 2023, Elsevier. p. 235-249.
[10] Özkaraca, O., et al., Multiple brain tumor classification with dense CNN architecture using brain MRI images. Life, 2023. 13(2): p. 349.
[11] Zhu, Z., S.-H. Wang, and Y.-D. Zhang, A survey of convolutional neural network in breast cancer. Computer modeling in engineering & sciences: CMES, 2023. 136(3): p. 2127.
[12] Gillmann, C., et al. Uncertainty-aware Visualization in Medical Imaging-A Survey. in Computer Graphics Forum. 2021. Wiley Online Library.
[13] Smarandache, F., A unifying field in Logics: Neutrosophic Logic, in Philosophy. 1999, American Research Press. p. 1-141.
[14] Smarandache, F., Neutrosophic masses & indeterminate models. Advances and Applications of DSmT for Information Fusion, 2015: p. 133.
[15] Kosko, B. and S. Isaka, Fuzzy logic. Scientific American, 1993. 269(1): p. 76-81.
[16] Zadeh, L.A., Fuzzy sets. Information and control, 1965. 8(3): p. 338-353.
[17] Salama, A., Basic structure of some classes of neutrosophic crisp nearly open sets and possible application to GIS topology. Neutrosophic Sets and Systems, 2015. 7: p. 18-22.

[18] Ali, M., I. Deli, and F. Smarandache, The theory of neutrosophic cubic sets and their applications in pattern recognition. Journal of intelligent & fuzzy systems, 2016. 30(4): p. 1957-1963.
[19] Guo, Y. and A.S. Ashour, Neutrosophic set in medical image analysis. 2019: Academic Press.
[20] Cai, G., et al., 14 - Neutrosophic set-based deep learning in mammogram analysis, in Neutrosophic Set in Medical Image Analysis, Y. Guo and A.S. Ashour, Editors. 2019, Academic Press. p. 287-310.
[21] Khalifa, N.E.M., et al., A study of the neutrosophic set significance on deep transfer learning models: An experimental case on a limited covid-19 chest x-ray dataset. Cognitive Computation, 2021: p. 1-10.
[22] Wajid, M.A., A. Zafar, and M.S. Wajid, A deep learning approach for image and text classification using neutrosophy. International Journal of Information Technology, 2024. 16(2): p. 853-859.
[23] Singh, S.K., V. Abolghasemi, and M.H. Anisi, Skin cancer diagnosis based on neutrosophic features with a deep neural network. Sensors, 2022. 22(16): p. 6261.
[24] Singh, S.K., V. Abolghasemi, and M.H. Anisi, Fuzzy logic with deep learning for detection of skin cancer. Applied Sciences, 2023. 13(15): p. 8927.
[25] Ieracitano, C., et al., A fuzzy-enhanced deep learning approach for early detection of Covid-19 pneumonia from portable chest X-ray images. Neurocomputing, 2022. 481: p. 202-215.
[26] Badawy, S.M., et al., Automatic semantic segmentation of breast tumors in ultrasound images based on combining fuzzy logic and deep learning—A feasibility study. PloS one, 2021. 16(5): p. e0251899.
[27] Breast-Histopathology-Images [Dataset], https://www.kaggle.com/datasets/paultimothymooney/breast-histopathology-images/discussion/202342, Editor. 2017.
[28] Dombi, J. and O. Csiszár, Modifiers and membership functions in fuzzy sets, in Explainable Neural Networks Based on Fuzzy Logic and Multi-criteria Decision Tools. 2021, Springer. p. 63-81.
[29] Olivas, E., et al., Chapter 11: Transfer Learning, Handbook of Research on Machine Learning Applications. 2009, IGI Publishing: Hershey, PA, USA.
[30] Simonyan, K. and A. Zisserman, Very deep convolutional networks for large-scale image recognition. arXiv preprint arXiv:1409.1556, 2014.
[31] He, K., et al. Deep residual learning for image recognition. in Proceedings of the IEEE conference on computer vision and pattern recognition. 2016.
[32] Huang, G., et al. Densely connected convolutional networks. in Proceedings of the IEEE conference on computer vision and pattern recognition. 2017.
[33] Tan, M. and Q. Le. Efficientnet: Rethinking model scaling for convolutional neural networks. in International conference on machine learning. 2019. PMLR.
[34] Sandler, M., et al. Mobilenetv2: Inverted residuals and linear bottlenecks. in Proceedings of the IEEE conference on computer vision and pattern recognition. 2018.
[35] Krizhevsky, A., I. Sutskever, and G.E. Hinton, Imagenet classification with deep convolutional neural networks. Advances in neural information processing systems, 2012. 25.
[36] Abadi, M., et al. {TensorFlow}: a system for {Large-Scale} machine learning. in 12th USENIX symposium on operating systems design and implementation (OSDI 16). 2016.
[37] Chollet, F., Deep learning mit python und keras: das praxis-handbuch vom entwickler der keras-bibliothek. 2018: MITP-Verlags GmbH & Co. KG.